Quadrature moments method for the simulation of turbulent reactive flows

By Venkatramanan Raman, Heinz Pitsch and Rodney O. Fox †

1. Motivation and Objectives

In recent years, computational fluid mechanics has become one of the primary tools for design and optimization of chemical reactors. With stringent environmental constraints, close control of product selectivity and an estimate of by-products are essential in successfully operating chemical plants. The fast throughput and enhanced mixing conditions offered by turbulent flows are increasingly exploited in chemical reactors. Viable simulation methods for such flows should be able to model the complex interaction of reaction and turbulent flow. All known reaction models used in these simulations follow a segregated approach where different techniques are used to solve the momentum and scalar transport equations. It is assumed that reaction affects fluid flow only through the change in density. Usually a variable density flow solver is utilized that accepts the density field from the scalar handler to correct the flow field. The scalar transport scheme uses the flow properties to evaluate the local density and this iterative procedure is used to advance the solution in time. The Eulerian solution technique that is commonly used in solving scalar transport equations inherently does not contain information about sub-grid level processes. The adverse effect of neglecting sub-grid scalar fluctuations in cases where the scalar evolves through non-linear rate expressions is well known. In combustion processes which are characterized by fast chemistry, use of flamelet model (Pitsch & Steiner 2000) or conditional moment closure (CMC) (Bilger 1993) based on a conserved scalar is known to be quite accurate in making qualitative as well as quantitative predictions. Such a method obviates the need for solving multiple scalar transport equations and is not restricted by the time-scale of individual reactions in the chemistry mechanism. The flamelet model, like all other reaction models, requires the specification of a scalar dissipation rate and assumes the shape of the PDF at the sub-grid level. The first-order CMC method models the conditional mean of the reacting scalars as a function of mixture fraction and local flow conditions. But the model ignores any fluctuations about the conditional mean and may not be viable in slow chemistry regimes. Both the CMC and flamelet model assume that all the reactive scalars can be parameterized by a single conserved scalar. On the other end of the spectrum, the transported-PDF scheme computes the sub-grid scalar-PDF in terms of a set of delta-functions. This method can be used in tandem with a flow solver like those based on the Reynolds-Averaged Navier Stokes (RANS) equation or Large-Eddy Simulation (LES) scheme to model reaction (Muradoglu *et al.* 1999; Haworth & El Tahry 1991). Such a formulation computes the profiles of all the species involved in the flow and leads to a closed form for the reaction source term. However, a mixing model is needed to describe the sub-grid mixing process and has been the focus of study in PDF methods (Subramaniam & Pope 1999; Valino 1995; Tsai & Fox

† Department of Chemical Engineering, Iowa State University

1998). The fact that no convincing mixing model exists is one of the important drawbacks of the method.

The transported-PDF still is an attractive scheme in that the reaction source term appears closed. The inhomogeneous transport equation for the sub-grid PDF is multi-dimensional and cannot be solved using Eulerian grid techniques. Particle based Monte-Carlo schemes used with realistic chemistry show good agreement with experimental results (Xu & Pope 2000; Masri & Pope 1990; Roekaerts 1991; Raman *et al.* 2003*a*). However, the handling of a large number of Lagrangian particles along with detailed chemistry can be computationally expensive. When using LES as the flow solver, such schemes can be outright intractable in practical flow configurations. In this work, an equivalent Eulerian version of the transported-PDF method is formulated for LES of reactive flows.

2. Filtered Quadrature Scheme for Variable Density Flows

For use in LES of reactive flows, a filtered density function (FDF) is defined (Gao & O'Brien 1993) that prescribes the sub-filter joint composition density function of the scalars.

$$F_L(\psi;\mathbf{x},t) = \int_{-\infty}^{+\infty} \rho(\mathbf{x}',t)\delta[\psi - \phi(\mathbf{x}',t)]G(\mathbf{x}'-\mathbf{x})d\mathbf{x}', \tag{2.1}$$

where F_L is the mass density function. This definition implies that in variable density flows, the FDF is the mass weighted and spatially filtered fine-grain density (Jaberi *et al.* 1999).

$$\int_{-\infty}^{+\infty} F_L(\psi;\mathbf{x},t)d\psi = \overline{\rho}, \tag{2.2}$$

where $\overline{\rho}$ is the filtered density. Using the scalar transport equation, the FDF is shown to evolve in multi-dimensional space as:

$$\frac{\partial F_L}{\partial t} + \frac{\partial\left[\overline{u}_i F_L\right]}{\partial x_i} = \frac{\partial}{\partial x_i}\left[(\gamma+\gamma_t)\frac{\partial\left(F_L/\overline{\rho}\right)}{\partial x_i}\right] + \frac{\partial}{\partial\psi_\alpha}\left[\Omega_m\left(\psi_\alpha - \overline{\phi}_\alpha\right)F_L\right] - \frac{\partial\left[S_\alpha F_L\right]}{\partial\psi_\alpha}, \tag{2.3}$$

where $\overline{u}_i$ is the Favre filtered velocity component, ψ is the composition array and $\overline{\phi}$ is the Favre filtered mean composition array. The molecular and turbulent diffusivities are denoted by γ and γ_t respectively. The mixing frequency is modeled as $\Omega_m = C_\Omega(\gamma+\gamma_t)/\left(\langle\rho\rangle_l \Delta_G^2\right)$, where Δ_G is the filter width. This high- dimensional equation is traditionally solved using Monte-Carlo schemes (Colucci *et al.* 1998; Raman *et al.* 2003*b*). As mentioned before, the particle based Monte-Carlo schemes are computationally expensive for large grids and hence become intractable even for simple chemistry. The Direct Quadrature Method of Moments (DQMOM) (Marchisio & Fox 2003; Wang & Fox 2003) is introduced here in the context of LES to provide an alternate tractable scheme.

Figure 1 shows the fine-grained PDF composed of a set of delta-functions approximating an arbitrary shaped PDF at a given point in the flow. Any particle based solution to the FDF equation will yield such an approximation. The FDF plot can be considered as a plot of normalized weights of particles in the computational cell. The accuracy of the approximation depends, among other factors, on the number of approximating delta functions. The N_α delta-functions are characterized by their positions ($\phi_{\alpha i}$) and their heights ($w_{\alpha i}$). The FDF is considered solved if for a given number of delta functions, the

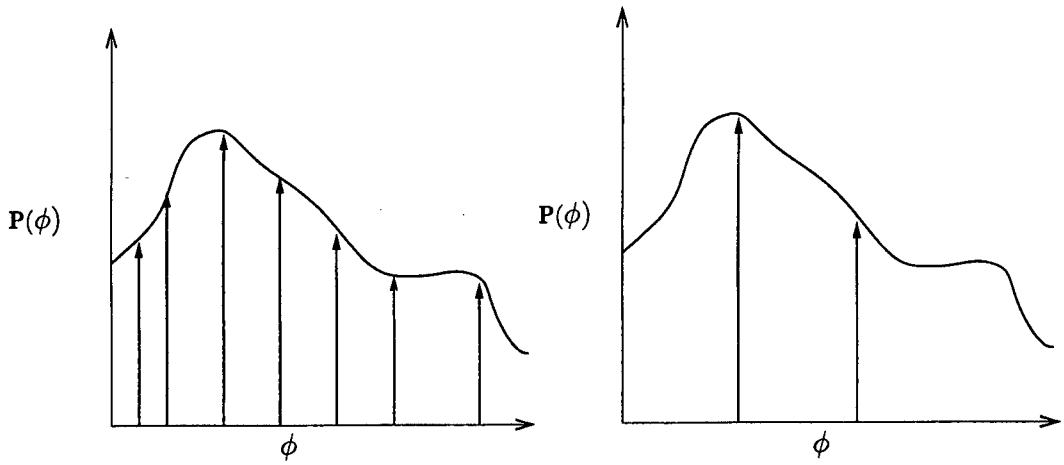

FIGURE 1. Approximation of a PDF using a finite number of delta functions. (Left) Transported PDF method and (Right) DQMOM method.

values of $\phi_{\alpha i}$ and $w_{\alpha i}$ are known. The DQMOM model formulates transport equations for these quantities based on pre-determined number of so-called environments, where each environment corresponds to a single delta-peak. The source terms involved in these equations ensure that the DQMOM equations match the moment equations of the scalar.

In the multi-environment DQMOM model, the FDF is assumed to be of the form:

$$F_L = \overline{\rho} \sum_{i=1}^{N} w_i \delta\left(\psi - \overline{\phi}_i\right). \tag{2.4}$$

The individual transport equations for the weights and locations of the delta-functions can be derived by substituting Eq. 2.4 into Eq. 2.3 (Fox 2003). For a single scalar case, this leads to

$$\begin{aligned}
&\sum_{i=1}^{N} \delta\left(\psi - \overline{\phi}_i\right) \left[\frac{\partial \overline{\rho} w_i}{\partial t} + \nabla \overline{\rho \mathbf{u}} w_i - \nabla \cdot (\Gamma + \Gamma_T) \nabla w_i\right] \\
&- \sum_{i=1}^{N} \delta^{(1)}\left(\psi - \overline{\phi}_i\right) \left\{\frac{\partial \overline{\rho} \overline{G}_i}{\partial t} + \nabla \overline{\rho \mathbf{u}} \overline{G}_i - \nabla \cdot (\Gamma + \Gamma_T) \nabla \overline{G}_i \right. \\
&\qquad \left. - \overline{\phi}_i \left[\frac{\partial \overline{\rho} w_i}{\partial t} + \nabla \overline{\rho \mathbf{u}} w_i - \nabla \cdot (\Gamma + \Gamma_T) \nabla w_i\right]\right\} \\
&- \sum_{i=1}^{N} \delta^{(2)}\left(\psi - \overline{\phi}_i\right) w_i (\Gamma + \Gamma_T) \nabla \cdot \nabla \overline{\phi}_i = R(\psi; \mathbf{x}, t),
\end{aligned} \tag{2.5}$$

where $\overline{G}_i = w_i \overline{\phi}_i$ and $R(\psi; \mathbf{x}, t)$ contains the mixing and reaction terms. $\delta^{(m)}$ indicates the m-th derivative of the delta function. The properties of δ function are used in rewriting the derivatives in terms of the filtered quantities (Pope 2000).

$$\frac{\partial \delta\left(\psi - \overline{\phi}\right)}{\partial t} = -\delta^{(1)}\left(\psi - \overline{\phi}\right) \frac{\partial \overline{\phi}}{\partial t} \tag{2.6}$$

and

$$\frac{\partial^2 \delta\left(\psi-\overline{\phi}\right)}{\partial x_j^2} = \delta^{(2)}\left(\psi-\overline{\phi}\right)\frac{\partial^2 \overline{\phi}}{\partial x_j^2}. \tag{2.7}$$

Following Fox (2003), Eq. 2.5 can be rewritten in terms of the transport equations for w_i and G_i, using a_i and b_i to denote the respective equations.

$$\sum_{i=1}^{N}\left[\delta\left(\psi-\overline{\phi}\right)+\overline{\phi}_i\delta^{(1)}\left(\psi-\overline{\phi}\right)\right]a_i - \sum_{i=1}^{N}\delta^{(1)}\left(\psi-\overline{\phi}\right)b_i = \sum_{i=1}^{N}\delta^{(2)}\left(\psi-\overline{\phi}\right)w_i c_i + R(\psi;\mathbf{x},t), \tag{2.8}$$

where $c_i = (\Gamma+\Gamma_t)(\nabla\overline{\phi}_i)^2$. In deriving these equations, the only assumption made so far is that the shape of the PDF is approximated by a finite-set of delta functions. For a N-environment model, $2N$ source terms need to be specified. It should be noted that if the number of scalars is more than one, several cross moments can also be specified. For details on the feasibility and choice of moments refer to Fox (2003) and Marchisio & Fox (2003). Here, only the pure moments, namely the mean and variance of a scalar are used in fixing the source terms. Multiplying Eq. 2.8 by ψ^m and integrating over the composition space yields:

$$(1-m)\sum_{i=1}^{N}\overline{\phi}^{m}{}_i a_i + m\sum_{i=1}^{N}\overline{\phi}^{m-1}{}_i b_i = m(m-1)\sum_{i=1}^{N}\overline{\phi}^{m-2}{}_i w_i c_i + R_m. \tag{2.9}$$

Similarly the reaction and mixing terms can be integrated to yield:

$$\begin{aligned} R_m &= \int_{-\infty}^{+\infty}\psi^m R(\psi;\mathbf{x},t) \\ &= -\int_{-\infty}^{+\infty}\psi^m\frac{\partial}{\partial\psi}\left\{\left[\Omega_m\left(\overline{\phi}-\psi\right)+S(\psi)\right]f_\phi\right\}d\psi \\ &= -m\int_{-\infty}^{+\infty}\psi^{m-1}\left\{\left[\Omega_m\left(\overline{\phi}-\psi\right)+S(\psi)\right]\sum_{i=1}^{N}\overline{\rho}w_i\delta\left(\psi-\overline{\phi}\right)\right\}d\psi \\ &= m\sum_{i=1}^{N}\overline{\rho}w_i\overline{\phi}_i^{m-1}\left\{\Omega_m\left(\overline{\phi}-\overline{\phi}_i\right)+S(\overline{\phi}_i)\right\}. \end{aligned} \tag{2.10}$$

Using Eqs 2.9 and 2.10 we can obtain the source terms a_i and b_i by solving a set of non-linear algberaic equations. In this work, N is set to two for all simulations. To further simplify the equations, we can arbitrarily set a_i to zero (Fox 2003). We then use $m = 1, 2$ to obtain the other source terms. Using the above moment equations, the non-linear system for b_i reduces to:

$$\begin{bmatrix}1 & 1\\ \phi_1 & \phi_2\end{bmatrix}\begin{bmatrix}b_1\\ b_2\end{bmatrix} = \begin{bmatrix}R_1\\ 2\left(w_1c_1+w_2c_2\right)+R_2\end{bmatrix}. \tag{2.11}$$

From the above set of equations, the source terms are determined to be:

$$a_1 = a_2 = 0, \tag{2.12}$$

$$b_1 = \frac{1}{\overline{\phi}_1 - \overline{\phi}_2} \sum_{i=1}^{2} w_i \Gamma_t (\nabla \overline{\phi}_i)^2 + \Omega_m \left(w_1 G_2 - w_2 G_1\right) + w_1 S(\phi_1), \tag{2.13}$$

and

$$b_2 = \frac{-1}{\overline{\phi}_1 - \overline{\phi}_2} \sum_{i=1}^{2} w_i \Gamma_t (\nabla \overline{\phi}_i)^2 - \Omega_m \left(w_1 G_2 - w_2 G_1\right) + w_2 S(\phi_2). \tag{2.14}$$

As discussed earlier, the number of environments can be considered to be equivalent to the particle number density used in a Lagrangian simulation. This implies that as the number of environments is increased, the accuracy of the scheme should increase (Wang & Fox 2003). The single scalar DQMOM can be extended to a multi-variate case using similar derivation technique (Fox 2003). In determining the source terms, one of the important criteria is that the pre-multiplier of the b vector in Eq. 2.11 is invertible. It should also be noted that a_i need not be set to zero and can be determined through a set of extended non-linear equations (Marchisio & Fox 2003).

3. Numerics

The numerical implementation for reactive flow simulations consists of two parts - the flow solver and the scalar handler. Here, we use a LES flow solver along with three different implementations of the scalar transport equation. The first method solves for the mean mixture fraction and reaction progress variable along with the variance of the mixture fraction using Eulerian transport equations for these quantities. The second method uses a Lagrangian Monte-Carlo scheme to solve the FDF of the mixture-fraction and reaction progress variable. The third implementation uses the DQMOM based 2-environment model to obtain the first and second moments of the scalars. In all these cases, the density field is obtained from the scalar handler and fed to the flow solver which corrects the flow according to reaction. To first establish the viability of the DQMOM model, we only consider reactions with no heat release in constant density incompressible flows and thus do not use the feedback loop. The flow solver provides the one-way transfer of velocity and turbulence fields to the scalar handler. The following subsections briefly explain the numerical implementations of each of the components.

3.1. *LES solver*

The second order LES scheme uses an energy conserving formulation for the momentum equations (Pierce 2001). The eddy viscosity and diffusivity are computed using dynamic Smagorinsky model (Moin *et al.* 1991). The LES scheme also solves for the scalar transport equation using a semi-implicit scheme. In the current work, scalar equations are solved for the mixture fraction Z and the reaction progress variable Y. The numerical implementation uses an upwind based QUICK scheme that is designed to reduce numerical oscillations but also leads to some amount of numerical dissipation.

For the sake of comparison, the mixture fraction variance transport equation is also simulated using production and dissipation terms consistent with the FDF formulation. Since sub-grid variance is a very small quantity in LES simulations, numerical dissipation can further increase the errors in the computation. To overcome this problem, a $\overline{Z} - \overline{Z^2}$ system is solved rather than the variance transport equation. The scalar equations are

obtained by integrating the FDF equation over mixture fraction space after multiplying by Z and Z^2.

$$\frac{\partial \overline{\rho} \widetilde{Z}}{\partial t} + \nabla \overline{\rho} \widetilde{\mathbf{U}} \widetilde{Z} = \nabla \left(\Gamma + \Gamma_T \right) \nabla \widetilde{Z} \tag{3.1}$$

$$\frac{\partial \overline{\rho} \widetilde{Z^2}}{\partial t} + \nabla \overline{\rho} \widetilde{\mathbf{U}} \widetilde{Z^2} = \nabla \left(\Gamma + \Gamma_T \right) \nabla \widetilde{Z^2} - \Omega_m \left(\widetilde{Z^2} - \widetilde{Z} \widetilde{Z} \right), \tag{3.2}$$

with Ω_m defined as before providing the time scale for scalar dissipation. This formulation ensures that in the limit of zero dissipation, the sub-grid variance is identical to the analytical solution:

$$\widetilde{Z''^2} = \widetilde{Z^2} - \widetilde{Z} = \widetilde{Z} \left(1 - \widetilde{Z} \right). \tag{3.3}$$

The inlet and boundary conditions for $\widetilde{Z^2}$ are identical to the filtered mixture fraction equation. This ensures that the sub-grid variance is zero at both the inlet and any boundaries in the domain. The chemical source term for the progress-variable equation is modeled based on the filtered means of the scalars and neglecting any sub-grid fluctuations. This "laminar" assumption leads to the following transport equation for the reactive scalar:

$$\frac{\partial \overline{\rho} \widetilde{Y}}{\partial t} + \nabla \overline{\rho} \widetilde{\mathbf{U}} \widetilde{Y} = \nabla \left(\Gamma + \Gamma_T \right) \nabla \widetilde{Y} + \overline{\rho} S(\widetilde{Y}). \tag{3.4}$$

The LES solution of the mixture fraction mean and variance equation provides an independent way of checking the transported PDF and DQMOM methods.

3.2. *Transported PDF solver*

In the Lagrangian implementation, the FDF transport equation is solved using an ensemble of notional particles. The hybrid composition-PDF scheme used here uses the flow fields from the LES solver (that was described in the previous section) to evolve stochastic particles that are evenly distributed in the entire computational domain. The evolution equations for the particles are obtained from Eq. 2.3 by using techniques similar to the RANS based hybrid method (Pope 1985; Colucci *et al.* 1998). The SDE's are solved for a system of particles which represents the FDF in composition space. The particles move in physical space according to:

$$d\mathbf{x}^* = \left(\widetilde{\mathbf{u}} + \frac{1}{\overline{\rho}} \nabla (\Gamma + \Gamma_t) \right) dt + \sqrt{2 \frac{(\Gamma + \Gamma_T)}{\overline{\rho}}} dW, \tag{3.5}$$

where $\mathbf{x}^*$ is the instantaneous position of the particle and dW represents the Wiener diffusion term. The motion in composition space is due to mixing and reaction.

$$d\boldsymbol{\phi}^* = \left[\Omega_m \left(\widetilde{\boldsymbol{\phi}} - \boldsymbol{\phi}^* \right) + \mathbf{S}(\boldsymbol{\phi}) \right] dt, \tag{3.6}$$

where $\boldsymbol{\phi}^*$ is the notional particle composition. Here the composition vector $\boldsymbol{\phi} = [Z, Y]$ evolves using reaction source terms $S(\boldsymbol{\phi}) = [0, S(Z, Y)]$. The use of the IEM model with the appropriate dissipation rate ensures that the variance dissipation is consistent with the LES solver. Since typical LES simulation use millions of computational cells, even a particle number density of 10-20 particles per cell will be computationally expensive. To ensure tractability, several novel computational algorithms are implemented. A pointer-based storage structure is used for handling the particles. Conventional algorithms use sorting procedures to keep the particles in order but are not feasible for such large numbers. Here an integer numbering procedure is used that uses pointer based linking of

particles to cells. Cells store only the index of the particles in their domain. Ownership of particles is transferred to the destination cell when particles move across faces. Such integer operations are inexpensive, even though they tend to loose some efficiency with iterations as the particles occupy discontinuous locations in memory. Particle motion is handled using an element-to-element tracking procedure (Subramaniam & Haworth 2000; Raman *et al.* 2003*a*). This algorithm splits the motion into a sequence of sub-steps that move individual particles from face-to-face with intermediate re-interpolation of particle velocity. Reflective boundaries can then be handled directly. In all the simulations carried out here, a nominal number density of 30 particles per cell is used. Particle splitting and merging is utilized to minimize the fluctuations in the number density. The details of the implementation and some preliminary results can be found in Raman *et al.* (2003*b*).

3.3. *DQMOM implementation*

The two-environment version of the model solves for the scalars w_1 ($w_2 = 1 - w_1$), $\overline{G}_{11}$, $\overline{G}_{12}$, $\overline{G}_{21}$, $\overline{G}_{22}$. The working set of equations can be written as

$$\frac{\partial \overline{\rho} w_1}{\partial t} + \nabla \overline{\rho \mathbf{u}} w_1 = \nabla \left(\Gamma + \Gamma_T\right) \nabla w_1. \tag{3.7}$$

$$\frac{\partial \overline{\rho} \overline{G}_{\alpha i}}{\partial t} + \nabla \overline{\rho \mathbf{u}} \overline{G}_{\alpha i} = \nabla \left(\Gamma + \Gamma_T\right) \nabla \overline{G}_{\alpha i} + S_{\alpha i}. \tag{3.8}$$

It can be seen that the evolution equation for the environment (Eq. 3.7) is identical to the mixture-fraction equation with no source term. The weighted scalar equations (Eq. 3.8) contain source terms that can be decomposed into mixing, reaction and correction components. These terms can be specified by first determining the location of the delta-functions in composition space in a given computational cell.

$$\overline{\phi}_{\alpha i} = \frac{\overline{G}_{\alpha i}}{w_i}. \tag{3.9}$$

The mixing source term takes the form:

$$S^m_{\alpha 1} = -S^m_{\alpha 1} = \Omega_m \left(w_{\alpha 1} \overline{G}_{\alpha 2} - w_{\alpha 2} \overline{G}_{\alpha 1}\right). \tag{3.10}$$

The correction term is obtained using the location of the delta peaks as

$$S^c_{\alpha 1} = -S^c_{\alpha 2} = \frac{1}{\overline{\phi}_{\alpha 1} - \overline{\phi}_{\alpha 2}} \sum_{i=1}^{2} (\Gamma_T + \Gamma) \left(\nabla \overline{\phi}_{\alpha i}\right)^2. \tag{3.11}$$

The reaction source term is computed based on the composition vector $\boldsymbol{\phi}_i$ in each environment as

$$S^r_{\alpha i} = S_\alpha \left(\overline{\boldsymbol{\phi}}_i\right). \tag{3.12}$$

The source term for the scalar equation $G\alpha i$ is then given by

$$S_{\alpha i} = S^m_{\alpha i} + S^c_{\alpha i} + w_i S^r_{\alpha i}, \tag{3.13}$$

where the reaction source term is multiplied by the weight in order to be consistent with the formulation.

The main implementation issue comes for the correction term. The correction term, $S^c_{\alpha 1}$, compensates for the excess moment source term arising from the finite-peak representation of the FDF. As seen above, this source term involves the inverse of the separation distance of the delta-peaks composition space. In regions of near-complete mixing,

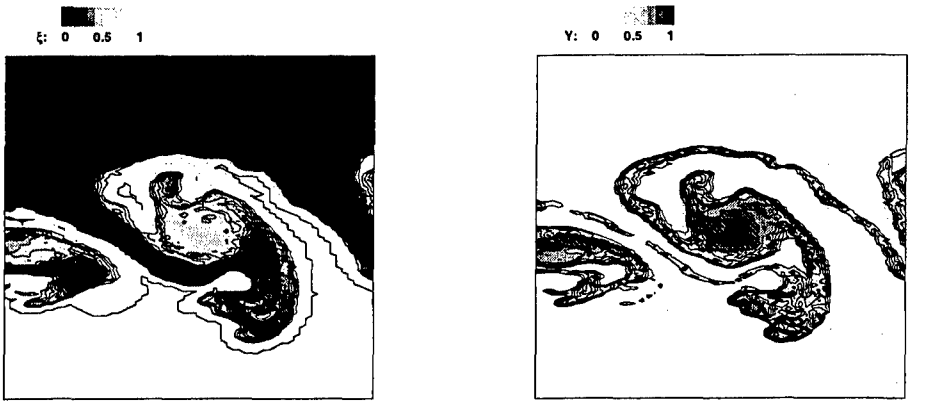

FIGURE 2. Instantaneous mixture fraction (left) and progress variable (right) contours simulated using the FDF scheme.

this term will approach zero leading to very large correction terms. Several alternatives have been suggested (Wang & Fox 2003) but in this work, an ad-hoc limit is used such that for all points where the difference $\phi_{\alpha 1} - \phi_{\alpha 2}$ is less than ϵ, this term is set to ϵ. Such an implementation using $\epsilon = 10^{-4}$ was found to be stable for all the cases studied.

Another important aspect to note is that the scalar solver does not maintain the bounds on the scalars. This might lead to peak locations outside the accessible range for the scalars. It was found that any attempt to limit these values led to a sharp decrease in the estimate of the variance. To counter this problem, for all grid cells that contain peaks outside the natural limits, the source terms were set to zero. The presence of reaction source terms with stiff kinetics was found to adversely affect this occurrence. Smaller time-steps that are determined based on reaction-time scale were found to alleviate this problem.

4. Simulations

The shear flow geometry of Mungal & Dimotakis (1984) is used to test the new scheme. The configuration consists of a planar shear layer formed by two streams entering at 8.8 m/s and 22 m/s velocity. Though the experiment involves a low heat-release fast chemistry, in this work we have not implemented this mechanism. Since the purpose is to compare different reaction models, a simple first order mechanism of the type $A+B \rightarrow P$ is used for modeling reaction. The rate expression is simplified using a mixture fraction-progress variable approach. Three different rate expressions that commonly occur in reacting flows are tested. The transported PDF scheme is also simulated for the same flow conditions and the results are compared with the DQMOM and LES simulations. A 256 $\times$ 128 grid spanning $80D$ in the axial direction and $40D$ in the cross-stream direction is used. Here D is set such that the observation point in the experiment is around $50D$. The inlet velocity profiles are assumed to be laminar with flat profiles. A development region corresponding to $10D$ extends into the domain where the two streams are separated by a splitter plate.

In all the simulations, the rate expression for the progress variable is of the form

$$r_Y = K\left(\frac{Z}{Z_{st}} - Y\right)\left(\frac{1-Z}{1-Z_{st}} - Y\right). \tag{4.1}$$

The rate constant K is varied to study the effect of non-linearity on DQMOM predictions. In the first case, the rate constant is set to a value of $K = 2$. Figure 2 shows the instantaneous mixture fraction and progress variable contours near the center of the domain. It shows the vortex like structure common to shear flows and the presence of highly mixed reactants at the center of such vortices. The peak in source term and mean progress variable are observed near the centerline. The vortices were found to stretch to a maximum of 10D in the cross-stream direction. It was found that the DQMOM model exhibits similar high reaction-rate zones. However, the LES simulations show a thick reaction zone with maximum allowable reaction rate at each location. In order to compare the steady-state trends, mean and variance of all scalars were time-averaged for at least one flow through time. Figure 3 shows the cross-stream profiles of the mixture fraction and sub-grid variance computed from all three schemes. Theoretically, the sub-grid variance obtained from all these methods should be identical. However, the differences in the implementation cause some discrepancy. Nevertheless, the time-averaged filtered mixture fraction and sub-grid variance predicted by all the schemes are in good agreement, thereby validating both the DQMOM and transported-PDF implementation.

The time-averaged mean and sub-grid variance of the reaction progress-variable obtained from the different schemes show some interesting features (Fig. 4). The sub-grid variance is non-zero only for the DQMOM and transported-PDF schemes and is set to zero for the LES scheme. In this context the LES solver can be considered as a one-environment model with complete sub-filter mixing. If the transported-PDF scheme is considered as a multi-environment DQMOM model, the particle scheme with a nominal number density of N represents an N-environment decomposition of the FDF. The cross stream profiles of the mean show that the DQMOM method provides a vast improvement over the one-environment solution. The mean profile shows that in spite of the simple rate expression, second moment terms cannot be neglected. The differences between the LES and DQMOM models are highest in the initial section where the effect of unmixed reactants will be very important. Since the inflow is laminar, the mixing layer itself does not become turbulent until about $X = 7.5$. However, the LES solver predicts very high reaction rates in even these laminar regions where low mixing should essentially keep the reaction rates to a very low value. This "early-ignition" is observed in the profiles at $X = 20$ where the mean value predicted by the LES solver is atleast 50% higher than that predicted by the DQMOM model. Surprisingly, the sub-grid variance profile from the DQMOM scheme also shows very good agreement with the PDF scheme. This essentially implies that the third and higher moments of the reactive scalar can be neglected for this chemistry scheme.

In the next case, a more complex rate expression is implemented. Reaction rates appearing in combustion have a strong dependence on temperature. Most source terms have an exponential dependence on local temperature. To simulate such a condition, the reaction rate constant was set to

$$K = 1000\exp\left(-\frac{b(1-Y)}{1-0.88(1-Y)}\right), \tag{4.2}$$

where b denotes the degree of dependence on temperature. For practical combustion

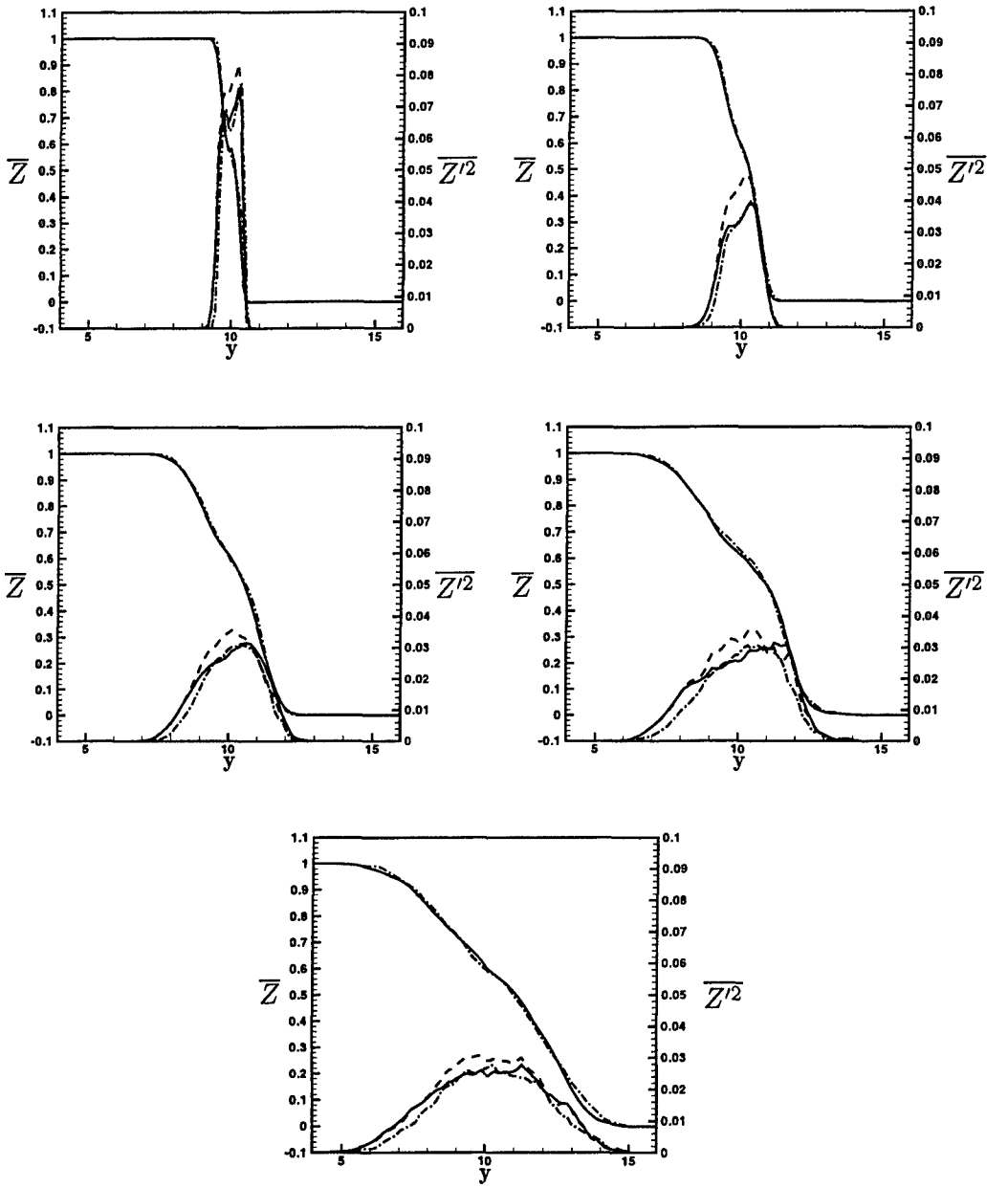

FIGURE 3. Comparison of time-averaged mean and variance of mixture fraction using a constant at different axial locations. (———) DQMOM, (----) LES and (—-—) PDF.

applications, b is usually set to values between 5 and 6. However, such high values lead to extinction for the present flow configuration. Instead, a lower value of 1 is chosen so that the reaction zone can be anchored near the splitter plate. This implies a weaker dependence on temperature but nevertheless makes the rate expression non-linear. Fig. 5 shows the cross-stream profiles of reaction progress variable. Here again, it can be seen

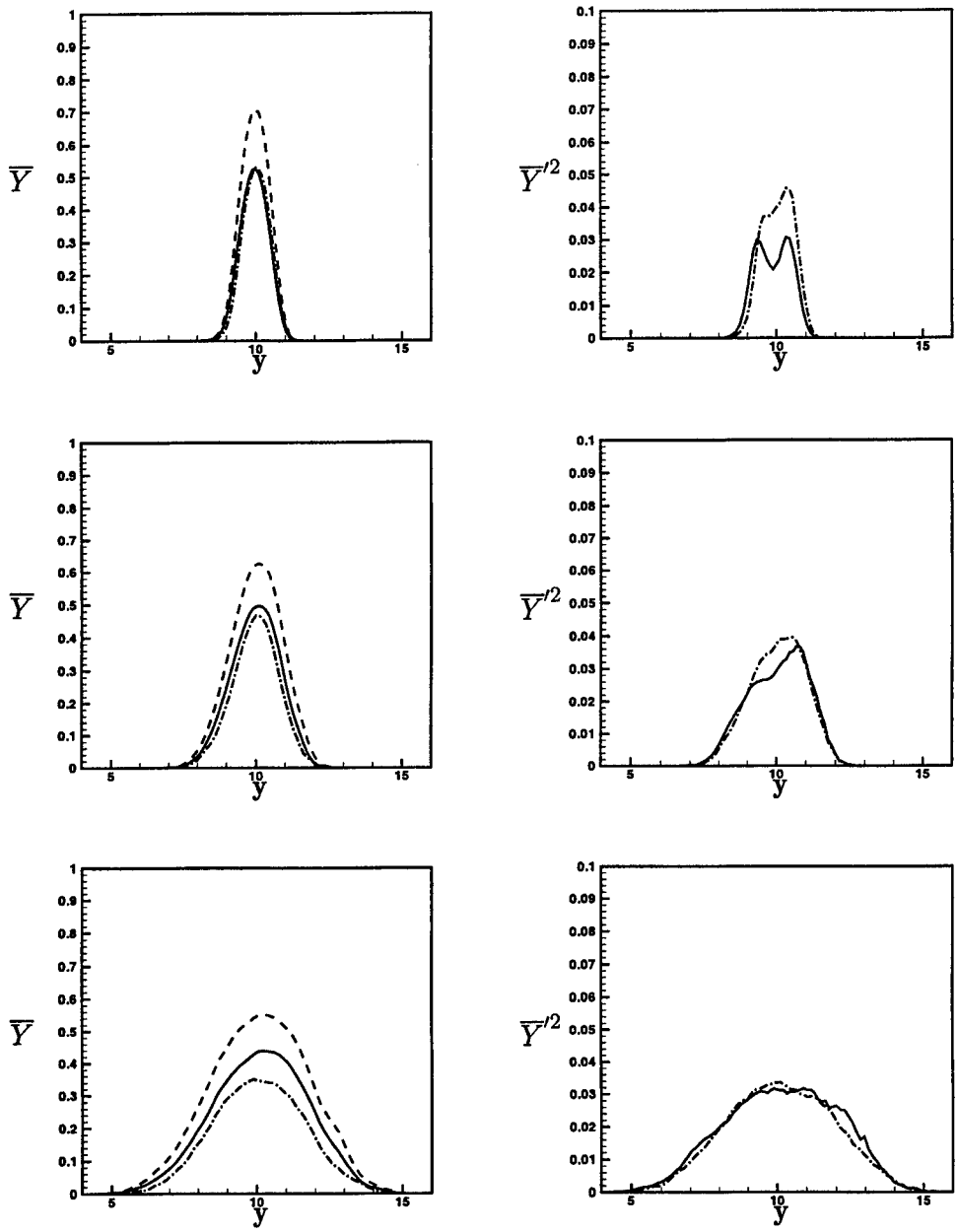

FIGURE 4. Comparison of time-averaged (left) mean and (right) variance of reaction progress variable using a constant rate constant at (top) X=20, (middle) X=30 and (bottom) X=50. (———) DQMOM, (- - - -) LES and (— - —) PDF.

that the DQMOM predictions of both the mean and the variance of the reactive scalar are in good agreement with the transported-PDF results. The LES predictions show fast rates consistent with the laminar assumption. It should be noted that depending on the reaction rates, the complete mixing assumption can also lead to quenching.

The third and final case uses a polynomial rate function which is common to chemical engineering assumptions. Reduced chemical mechanisms like the chloromethane reactions (West *et al.* 1999) may even involve non-integer moments of the scalar variable. Here, the rate is defined as

$$r_Y = 1000\frac{0.0001 + Y^2}{1.0 + Y}. \tag{4.3}$$

This expression ensures that the reaction proceeds without the need for an ignition source. The predicted mean and variance (Fig. 6) indicate good agreement with the transported-PDF scheme. This clearly shows that the DQMOM model with just two environments is able to drastically improve the single-environment predictions obtained from the LES solver.

In terms of computational requirements, the particle based transported-PDF solver was nearly 5 times slower than the DQMOM scheme even for such simple geometries. For complex configurations, the memory requirements of a large ensemble of particles can further slow down the simulation. However, the DQMOM scheme it not without limitations. In particular, the time-scale limitations of a stiff-chemistry source term can reduce the time-step used in the DQMOM model while the robust chemistry solvers (e.g ISAT (Pope 1997)) can increase the computational speed of the transported-PDF model. In addition, detailed chemistry mechanisms will require a large number of scalar transport equations and may eventually diminish the advantages over the particle scheme. In spite of these observations, present study shows that the DQMOM scheme is a viable altrernative to the Monte-Carlo based transported-PDF model and needs to be further explored for multi-species systems.

5. Conclusions and Future Work

A sub-filter model for reactive flows, namely the DQMOM model, was formulated for LES using the filtered mass density function. Transport equations required to determine the location and size of the delta-peaks were then formulated for a 2-peak decomposition of the FDF. The DQMOM scheme was implemented in an existing structured-grid LES solver. Simulations of scalar shear layer using an experimental configuration showed that the first and second moments of both reactive and inert scalars are in good agreement with a conventional Lagrangian scheme that evolves the same FDF. Comparisons with LES simulations performed using laminar chemistry assumption for the reactive scalar show that the new method provides vast improvements at minimal computational cost.

Currently, the DQMOM model is being implemented for use with the progress variable/mixture fraction model of Pierce (2001). Comparisons with experimental results and LES simulations using a single-environment for the progress-variable are planned. Future studies will aim at understanding the effect of increase in environments on predictions.

REFERENCES

BILGER, R. W. 1993 Conditional moment closure for turbulent reacting flow. *Physics of Fluids* **5** (2), 436–444.

COLUCCI, P. J., JABERI, F. A. & GIVI, P. 1998 Filtered density function for large eddy simulation of turbulent reacting flows. *Physics of Fluids* **10** (2), 499–515.

FOX, R. O. 2003 Computational Models for Turbulent Reactive Flows. Cambridge University Press, To be published.

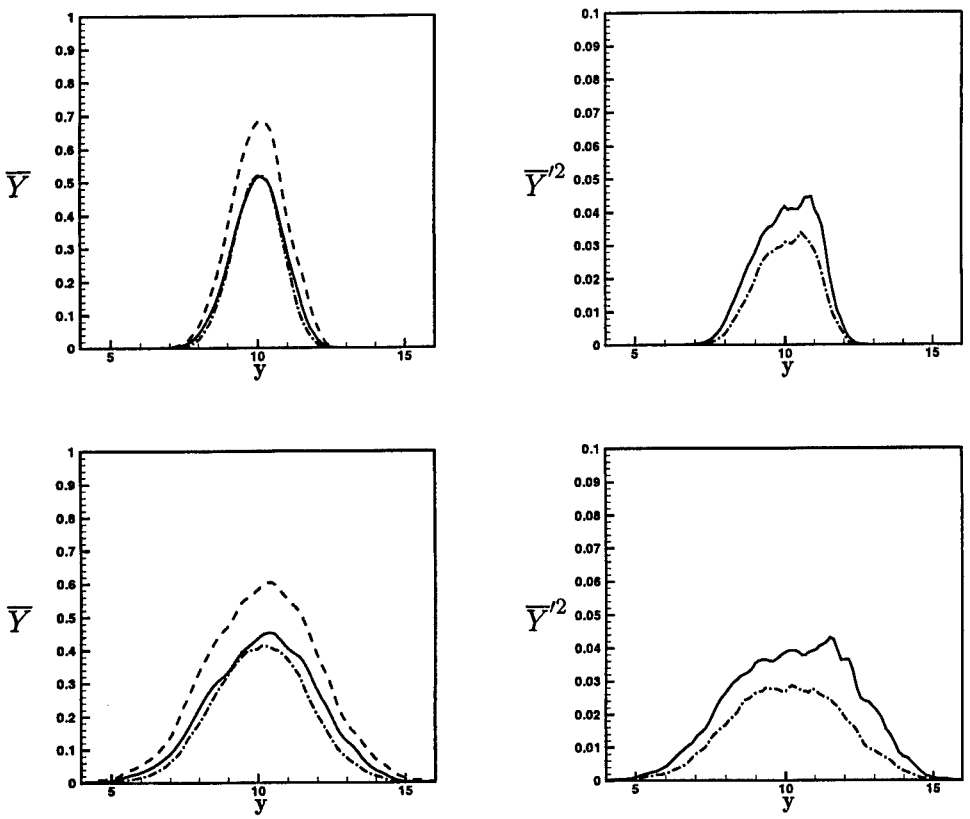

FIGURE 5. Comparison of time-averaged (left) mean and (right) variance of reaction progress variable for exponential reaction rate at (top) X=30 and (bottom) X=50. (———) DQMOM, (----) LES and (—·—) PDF.

GAO, F. & O'BRIEN, E. E. 1993 A large-eddy simulation scheme for turbulent reacting flows. *Physics of Fluids* **5** (6), 1282.

HAWORTH, D. C. & EL TAHRY, S. H. 1991 Probability density function approach for multidimensional turbulent flow calculations with application to in-cylinder flows in reciprocating engines. *AIAA Journal* **29** (2), 208–218.

JABERI, F. A., COLUCCI, P. J., JAMES, S., GIVI, P. & POPE, S. B. 1999 Filtered mass density function for large-eddy simulation of turbulent reacting flows. *Journal of Fluid Mechanics* **401**, 85–121.

MARCHISIO, D. L. & FOX, R. O. 2003 Direct quadrature method of moments: Derivation, analysis and applications. *Submitted to Journal of Computational Physics.*

MASRI, A. R. & POPE, S. B. 1990 Pdf calculations of piloted turbulent nonpremixed flames of methane. *Combustion and Flame* **81** (1), 13–29.

MOIN, P., SQUIRES, K., CABOT, W. & LEE, S. 1991 A dynamic subgrid-scale model for compressible turbulence and scalar transport. *Physics of Fluids A* **3**, 2746–2757.

MUNGAL, M. & DIMOTAKIS, P. E. 1984 Mixing and combustion with low heat release in a turbulent mixing layer. *Journal of Fluid Mechanics* **148**, 349–382.

MURADOGLU, M., JENNY, P., POPE, S. B. & CAUGHEY, D. A. 1999 A consistent

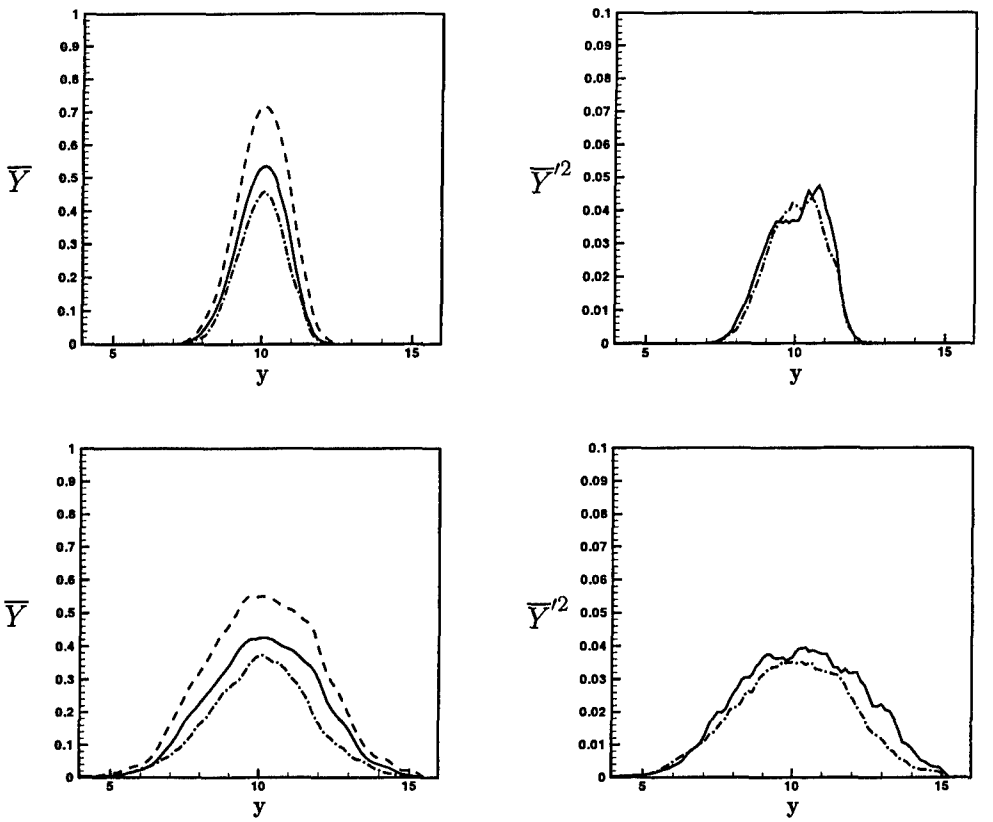

FIGURE 6. Comparison of time-averaged (left) mean and (right) variance of reaction progress variable for polynomial reaction rate at (top) X=30 and (bottom) X=50. (———) DQMOM, (----) LES and (—-—) PDF.

hybrid finite-volume/particle method for the PDF equations of turbulent reactive flows. *Journal of Computational Physics* **154**, 342–371.

PIERCE, C. D. 2001 Progress-variable approach for large-eddy simulation of turbulence combustion. PhD thesis, Stanford University.

PITSCH, H. & STEINER, H. 2000 Large-eddy simulation of a turbulent piloted methane/air diffusion flame (sandia flame D). *Physics of Fluids* **12** (10), 2541–2554.

POPE, S. B. 1985 PDF methods for turbulent reactive flows. *Progress in Energy and Combustion Science* **11**, 119.

POPE, S. B. 1997 Computationally efficient implementation of combustion chemistry using in-situ adaptive tabulation. *Combustion Theory Modelling* **1**, 41.

POPE, S. B. 2000 *Turbulent Flows*. Cambridge University Press.

RAMAN, V., FOX, R. O., HARVEY, A. D. & WEST, D. H. 2003*a* Effect of feed-stream configuration on gas-phase chlorination reactor performance. *Industrial and Engineering Chemistry Research* **42**, 2544–2557.

RAMAN, V., PITSCH, H. & FOX, R. O. 2003*b* Hybrid LES-PDF methods for the simulation of turbulent reactive flows. *To appear in Proceedings of the Topical Conference on Computers at Work, AIChE Annual Meeting, San Francisco, 2003*

ROEKAERTS, D. 1991 Use of a Monte Carlo PDF method in a study of the influence of turbulent fluctuations on selectivity in a jet-stirred reactor. *Applied Scientific Research* **48**, 271.

SUBRAMANIAM, S. & HAWORTH, D. 2000 A PDF method for turbulent mixing and combustion on three-dimensional unstructured deforming meshes. *International Journal of Engine Research* **1**, 171–190.

SUBRAMANIAM, S. & POPE, S. B. 1999 Comparison of mixing model performance for non-premixed turbulent reactive flow. *Combustion and Flame* **117**, 732.

TSAI, K. & FOX, R. O. 1998 The BMC/GIEM model for micromixing in non-premixed turbulent reacting flows. *Industrial Engineering Chemistry Research* **37** (6), 2131–2141.

VALINO, L. 1995 Multiscalar mapping closure for mixing in homogeneous turbulence. *Physics of Fluids* **7**, 144.

WANG, L. & FOX, R. O. 2003 Comparison of micromixing models for CFD simulation of nanoparticle formation by reactive precipitation. *Submitted to AIChE Journal.*

WEST, D. H., HEBERT, L. A. & PIVIDAL, K. A. 1999 Detection of quenching and instability in industrial chlorination reactors. In *Fall AIChE Annual Meeting*. Dallas.

XU, J. & POPE, S. B. 2000 Pdf calculations of turbulent nonpremixed flames with local extinction. *Combustion and Flame* **123**, 281–307.